Appl. Sci. Converg. Technol. 26(6): 174-178 (2017)
http://dx.doi.org/10.5757/ASCT.2017.26.6.174

Research Paper

Surface Reactions of Atomic Hydrogen with Ge(100) in Comparison with Si(100)

Sam Keun Jo*
Department of Nanochemistry, Gachon University, KyungKi 13120, South Korea

Received November 6, 2017; revised November 22, 2017; accepted November 24, 2017

Abstract The reactions of thermal hydrogen atoms H(g) with the Ge(100) surface were examined with temperature-programmed desorption (TPD) mass spectrometry. Concomitant H_2 and CH_4 TPD spectra taken from the H(g)-irradiated Ge(100) surface were distinctly different for low and high H(g) doses/substrate temperatures. Reactions suggested by our data are: (1) adsorbed mono(β_1)-/di-hydride(β_2)-H(a) formation; (2) H(a)-by-H(g) abstraction; (3) GeH_3(a)-by-H(g) abstraction (Ge etching); and (4) hydrogenated amorphous germanium *a*-Ge:H formation. While all these reactions occur, albeit at higher temperatures, also on Si(100), H(g) absorption by Ge(100) was not detected. This is in contrast to Si(100) which absorbed H(g) readily once the surface roughened on the atomic scale. While this result is rather against expectation from its weaker and longer Ge-Ge bond as well as a larger lattice constant, we attribute the absence of direct H(g) absorption to insufficient atomic-scale surface roughening and to highly efficient subsurface hydrogenation at moderate (>300 K) and low (≤300 K) temperatures, respectively.

Keywords: Ge(100) Surface Adsorption, Surface Etching, Hydrogen Adsorption, Subsurface Hydrogenation

I. Introduction.

The chemistry of gaseous hydrogen atoms, H(g), on and in crystalline group-IV semiconductors has been an active research area for decades [1-7]. Reactions that occur, when H(g) is exposed to Si(100), have thus been well documented: surface-adsorbed mono- and di-hydride formation [6-7]; H(a)-by-H(g) abstraction [8]; surface etching as a result of the SiH_3(a)-by-H(g) abstraction [11]; amorphous hydride (*a*-Si:H) formation from subsurface hydrogenation [12]; and direct absorption of H(g) by the crystalline bulk [8,13]. The relative importance of theses reactions is determined mostly by the substrate temperature. While the surface etching of Si(100) by H(g) is slow and anistropic at moderately elevated temperatures, it becomes faster and rather isotropic at room temperature [8,9]. At even lower temperatures, subsurface Si(100) hydrogenation/amorphization is a dominant reaction channel [12]. The Si(100) surface becomes rougher on the atomic sale at elevated temperatures as a result of anisotropic etching by H(g) [9]. It was found that the surface roughened by H(g) etching provides a low-barrier channel for direct H(g) absorption by Si(100) [8]. H atoms incorporated into crystalline silicon (*c*-Si) deactivates dopants, other impurities, and lattice vacancy defects, profoundly affecting fabricated Si devices [1-5,14].

On the other hand, much less research attention has been paid to the surface chemistry of H(g) on Ge(100) compared with Si(100) [15-19]. While germanium attracts renewed attention in view of the next-generation semiconductor technology due to its high carrier mobility [20-30], we decided to perform a comparative study on the H(g)/Ge(100) system. Compared with *c*-Si, *c*-Ge has a larger lattice constant and a weaker Ge-Ge bond on average.

We hereby report the effects of substrate temperature and exposure on the surface reactions of H(g) on Ge(100) in comparison with the previous results for Si(100). Similarly, H(g) adsorption to form surface mono- and di-hydrides, H(a)-by-H(g) abstraction, GeH_3(a)-by-H(g) etching, and sub-surface hydrogenation all occurred, albeit at lower temperatures. In contrast to Si(100), however, no absorption of H(g) has been detected even with extremely large H(g) exposures on Ge(100) despite its larger lattice constant (more spacious interstices) and its weaker bond strengths (facile hydrogenation and/or etching). We discuss this difference and propose a plausible explanation for the lack of expected H(g) absorption.

II. Experimental.

Experiments were carried out in a turbo-molecular pumped ultrahigh vacuum (UHV) system with a base pressure of 4×10^{-11} Torr. The main 500 L/s turbo pump was backed by a 500 L/s oil diffusion pump and in turn by a mechanical pump. The UHV system was equipped with a single-pass cylindrical mirror analyzer (PHI 3017 model)

*Corresponding author
E-mail: samjo@gachon.ac.kr

for the Auger electron spectroscopic (AES) analysis of surface elemental compositions, a differentially pumped triple-filter quadrupole mass spectrometer (QMS, and Thermo-Fisher Scientific Smart IQ + 300D) for residual gas analysis (RGA) and for temperature-programmed desorption (TPD) measurements of desorbing species from the sample surface. The experimental system was also equipped with a high-purity gas delivery system with a tubular gas doser connected to a precision leak valve.

The Ge(100) sample used here was p-type (B-doped; ρ = 0.01~0.39 ohm-cm) and cut into a 10 × 18 mm^2 piece. It was then mounted on an XYZ-rotational manipulator for liquid nitrogen sample cooling, electrical feedthroughs for *dc* resistive sample heating for TPD measurements, and a type-K thermocouple inserted and glued (Aremco 516 high-temperature ceramic adhesive) into a small hole drilled on the sample edge for accurate T_s measurements. The sample temperature (T_s) was regulated precisely by a *dc* power supply, which is in turn controlled for a linear temperature ramping by an electronic temperature programmer (Eurotherm 2404) interfaced to PC control software.

The sample, introduced into our UHV chamber without pretreatment, was cleaned *in situ* with several cycles of a 30-min 1-keV Ar+-ion sputtering at 700 K and a subsequent 10-min annealing at 900 K. H_2 gas (99.999 purity) was introduced into the chamber through a tubular doser controlled by a pinhole disc. Thermal-energy hydrogen atoms H(g) were produced by a hot (~1800 K) spiral W filament positioned ~6 mm in front of an H_2 gas dosing tube facing the sample surface from a distance of 3 cm. H(g) exposures are reported here in monolayers (ML), calibrated against the exposure of 155-L H_2 to give a saturation monohydride coverage, Ge(100)-2 × 1:H. Following each H(g) dose, the sample was rotated 90° away from the tubular gas doser and positioned in front of a 3 mm diameter apertured cone to face the differentially pumped QMS from a line-of-sight distance of 1 mm. TPD measurements were made with a 2.5 K/s ramp rate. Ultrahigh-purity (99.999%) H_2 gas was further purified with a liquid nitrogen trap in a turbo-pumped (<2 × 10^{-7} Torr) gas manifold and checked for impurity gases with RGA.

III. Results and Discussion.

It has been well established that both Si(100) and Ge(100) surfaces reconstruct to make (2Í1) surfaces, on which each surface atom has only one dangling bond. Such dangling bonds are readily passivated by H(g) with a nearly unity sticking probability, leading to well-ordered monohydride-saturated surfaces, Si(100)-2 × 1:H [8-12] and Ge(100)-2 × 1:H [16-19,27-28]. Schematic views of the unit cell of a diamond crystal lattice and the (100)-2 × 1:H surface are drawn in Figure 1. Surface dimer bonds on these (100)-2x1:H (1 ML θ_H) surfaces are strained (weak) and are vulnerable to the attack of H(g) to make a (100)-3x1:H (1.33 ML θ_H) phase, which is composed of alternating monohydride dimer and dihydride rows. Both the interatomic distances on the surface (labelled A and B in the Figure 1) and the lattice constant are *larger* by ~4%

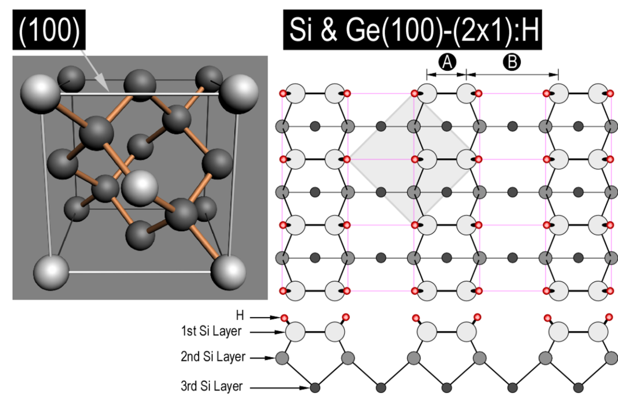

Figure 1. Model views for the diamond crystal lattice unit cell and the (2 × 1)-reconstructed (100) surface with all dangling bonds passivated each with an H atom. The intra- (A) and inter-dimer (B) Si-Si (Ge-Ge) distances are 2.3 Å (2.4 Å) and 5.38 Å (5.58 Å), respectively, on their (100)-2Í1 surfaces. The lattice constants are 5.431 Å and 5.646 Å for Si and Ge, respectively.

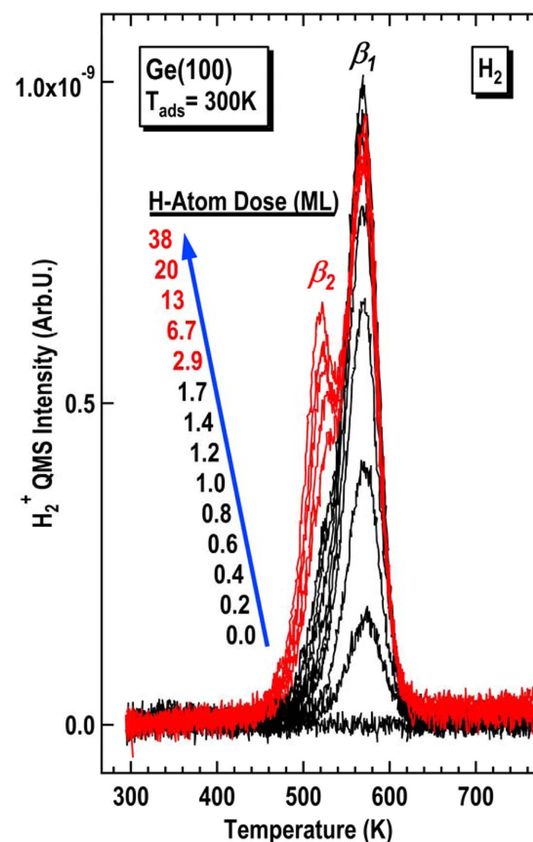

Figure 2. H_2 TPD Spectra from the Ge(100) surface pre-exposed to atomic H at 300 K in the *low* exposure regime. The 1-ML atomic H dose, calibrated against the saturation β_2-peak intensity, corresponds to a 155-L H_2 dose in front of a hot (~1800 K) spiral tungsten filament.

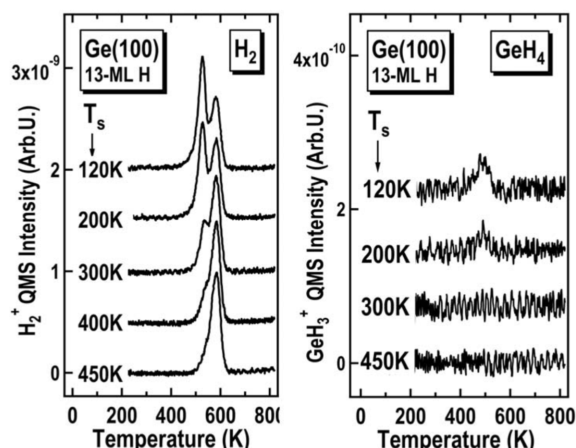

Figure 3. H_2 (Left Panel) and GeH_4 (Right Panel) TPD spectra simultaneously taken from the Ge(100) surface pre-exposed to a fixed 13-ML atomic H(g) at the indicated surface temperatures.

for Ge(100). On average, Ge-Ge and Ge-H bonds are *weaker* and *longer* than the corresponding Si-Si and Si-H bonds. With these structural and chemical similarities and differences in mind, we analyze and compare our results for Ge(100) obtained in this work with the literature results in terms of various reaction channels as functions of the substrate temperature T_s and the H(g) dose.

Displayed in Figure 2 is a series of low-dose H_2 TPD spectra taken from the Ge(100)-2 × 1 surface pre-exposed to indicated H(g) exposures (ML) at 300 K. The red-colored desorption curves are those with an additional shoulder peak (labelled β_2 at 520 K) indicative of dihydrides, GeH_2(a), which grows beyond the primary peak (β_1 at 570 K) for monohydrides, GeH(a). Similar double-peaked desorption behaviors have been reported for both Si(100) [8-12] and Ge(100) surfaces [8-12,16-19,27-28]. However, there is one distinct aspect observed here: the β_2-peak grew, albeit relatively slowly compared with Si(100), well beyond the 1.33-ML H(a) coverage corresponding to a (3 × 1):H phase on Ge(100) (see Figure 3).

A strong dependence on the surface temperature (T_s) was observed as summarized in Figure 3. The β_2-H_2 desorption peak, which is H_2 desorption from surface dihydride GeH_2(a) species, increases sharply with decreasing T_s for a fixed dose of 13-ML H(g). Together with the 500-K GeH_4 desorption (See the right panel of Figure 3), the strong β_2-H_2 peak intensities obtained with $T_s \leq 300$ K indicate the formation of surface multi-hydrides GeH_x(a) (x = 2 and 3) and surface etching. It was previously shown that Si etching via SiH_3(a)-by-H(g) abstraction during H(g) dose also occurs at adsorption T_s that leads to strong β_2-H_2 and SiH_4 desorption in TPD [8-10,31]. The detection of GeH_4 TPD peak at 490 K, resulting from the recombination of two surface adsorbates, SiH_3(a) and H(a), suggests that SiH_3(a) species are formed and abstracted by H(g) during the H(g) dose. We thus conclude that H(g) atoms, when exposed to Ge(100) at T_s below 300 K, not only form surface GeH_x(a) (x > 1) species but also abstract GeH_3(a) to produce the gaseous etch product GeH_4 from Ge(100) during H(g) dose. A very similar behavior was observed on Si(100), although the threshold T_s is about 200 K lower on Ge(100) [8-11,16-18,31]. It should be noted that the β_2-H_2 peak grows at the sacrifice of the β_1-H_2 peak with decreasing T_s: The β_1-peak intensity decreased by ~33% when T_{ads} decreased from 450 K to 120 K. This suggests that the increase of the total H_2 desorption with decreasing T_{ads} was due to the increased concentration of increased di- and tri-hydrides on the surface, rather than to etching-induced roughening and a subsequent increase in the area of the surface.

The evolution of H_2 desorption peaks, as a function of H(g) exposure in the high-dose regime at low surface temperatures (T_{ads} = 120, 200, and 300 K), is shown in Figure 4. Noteworthy features are: (1) the β_2-to-β_1 peak intensity ratio for a given dose of 13-ML H(g) increases with decreasing T_s; (2) the amount of overall H_2 desorption

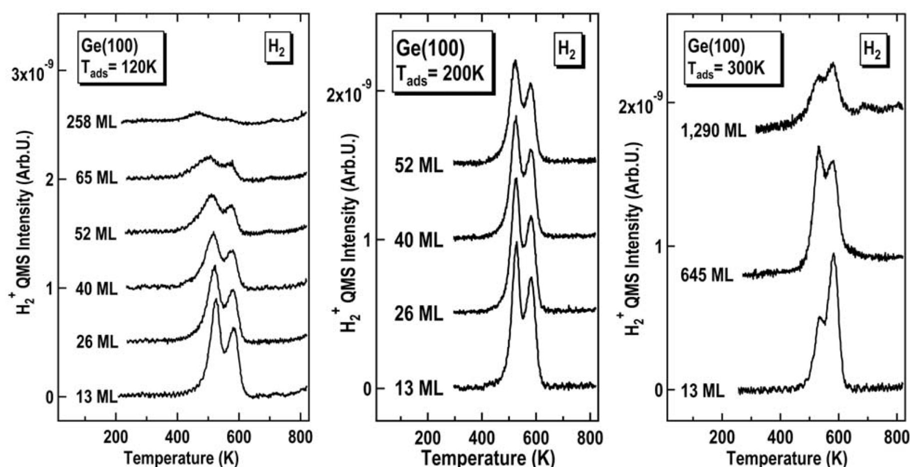

Figure 4. H_2 TPD spectra from the Ge(100) surface pre-exposed to the indicated amounts of H(g) atoms (in ML) at three different (T_{ads} = 120, 200, and 300 K) surface temperatures. Note that the β_2-to-β_1 H_2 peak intensity ratio increases with the decreasing surface dosing temperature and that both β_1- and β_2-H_2 peak intensities diminish with the increasing H(g) dose more quickly at lower substrate temperatures during dose.

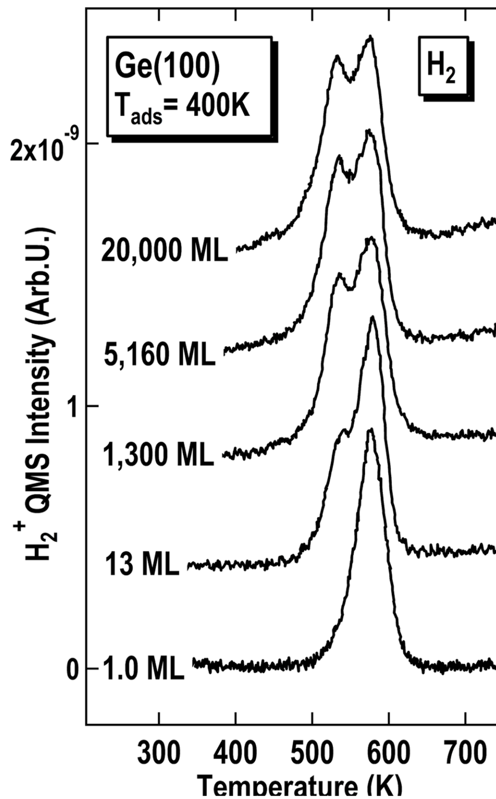

Figure 5. H_2 TPD spectra taken from the Ge(100) surface pre-exposed to H atoms at a fixed surface temperature of 400 K. Note that the trend of the decreasing H_2 desorption, observed at lower dosing temperatures, does not take place and that the β_2-desorption peak rather increases, albeit slowly, steadily to reach ~1.5 ML of a total H uptake.

decreases with increasing H(g) dose; and (3) the H_2 desorption decreases more quickly at a lower T_{ads} with increasing H(g) dose. Previously, very similar results were obtained from Si(100) at T_s between 115 and 300 K [12]. Low-energy electron diffraction (LEED) and TPD analyses revealed that hydrogenation proceeds beyond the topmost surface atoms, forming amorphous hydrogenated Si layers, *a*-Si:H, in the subsurface of Si(100). We thus conclude that a large H(g) dose at a low $T_s \leq 300$ K leads to subsurface hydrogenation of Ge(100). The nearly complete suppression of both β_1- and β_2-H_2 desorption (see the top curve on the left panel), together with increased desorption of GeH_x (x < 4) species in TPD (not shown), is ascribed to *a*-Ge:H formation on Ge(100) [12]. The quicker decrease in H_2 desorption at a lower T_s suggests that the subsurface hydrogenation occurs more rapidly at lower T_s. From comparison with Si(100) [12], it is also concluded that Ge(100) is hydrogenated more readily and to a greater extent than Si(100). The difference might be reconciled with the weaker and longer Ge-Ge and Ge-H bonds and with the larger lattice constant of Ge(100).

Figure 5 shows H_2 TPD spectra taken from the Ge(100) surface pre-exposed to very large H(g) doses at 400 K. The β_1-H_2 peak intensity maximizes at a 1-ML H(g) and then decrease slowly with increasing H(g) exposure up to 20,000 ML. The decreasing β_1-H_2 intensity parallels the increasing β_2-H_2 desorption. This trend was common for T_{ads} down to 120 K, as can be seen in Figure 4. Moreover, the β_2/β_1 peak intensity ratio is smaller than those of low-T_{ads} H(g) doses, suggesting that etching would occur mostly a step edge sites, leading to slow but anisotropic surface etching. However, the total (β_1- and β_2-) H_2 desorption increased only by ~15% from 1-ML to 20,000-ML H(g). This very small increase suggests that GeH_3(a)-by-H(g) etching occurs too slowly to result in a significant increase in the surface area on Ge(100). This is in sharp contrast with Si(100), where anisotropic etching dominates at moderate temperatures, leading to a roughened surface with a more than doubly increased area, estimated by the total H_2 desorption of surface-bound H(a) [8]. Once roughened significantly by etching by H(g), the Si(100) surface directly absorbed H(g) unlimitedly within a 400-600 K T_s window. H(g) atoms absorbed by the crystalline bulk of Si(100) evolved out as strong H_2 peak at 860-900 K, well-resolved from the 780-K β_1- and 650-K β_2-H_2 desorption peaks for surface-bound hydrogen atoms [8,10].

From the absence of no additional H_2 TPD peak even with an extremely large H(g) dose of 20,000 ML, except the well-known β_1- and β_2-H_2 peaks for surface-adsorbed H(a), we conclude that the crystalline bulk of Ge(100) does not absorb H(g). This suggests that the Ge(100) surface also needs to be pre-roughened significantly on the atomic scale for direct H(g) absorption into the Ge(100) lattice bulk to occur. This result is rather surprising when the larger lattice constant of Ge(100), together with longer and weaker Ge-Ge and Ge-H bonds on average, is considered. Weber et al. [20] also suggested an effective diffusion barrier for atomic H to explain the low H concentration incorporated in the crystalline bulk of germanium from a hydrogen plasma. Both atomic and molecular H_2 are important in preparation and chemical processing of semiconductor surfaces [19,24-28]. Isolated H atoms play an important role of passivating imperfections in the crystalline lattice of semiconductors in the manufacture of electronic devices [32-33]. While the insufficient surface roughening and/or anisotropic etching with the much greater H(g) is concluded to be the lack for the bulk H(g) absorption by Ge(100) in this work, further studies with a pre-roughened, e.g., HF-etched, Ge(100) surface would confirm our conclusion [10].

IV. Summary

Reactions of atomic hydrogen H(g) with the Ge(100) surface were investigated as a function of surface temperature and H(g) dose. While all surface reactions, i.e., adsorption, abstractive surface etching, and subsurface hydrogenation and amorphization, that occur on Si(100) were confirmed to take place also on Ge(100), direct H(g) absorption by Ge(100) was not detected for wide ranges of

substrate temperatures and H(g) doses. The larger lattice constant and weaker Ge-Ge bond were not enough to provide a low-barrier surface channel for direct H(g) absorption. We attribute the absence of H(g) absorption to an insufficient surface roughening of the Ge(100) surface at $T_s > 300$ K and to predominantly occurring subsurface hydrogenation, forming amorphous germanium hydride *a*-Ge:H layers, at $T_s \leq 300$ K.

Acknowledgement

SKJO thanks Dr. Minbok Jung for his help in carrying out early experiments.

References

[1] M. Stutzmann and J. Chevallier (Ed.), *Hydrogen in Semiconductors: Bulk and Surface Properties* (North-Holland, Amsterdam, 1991).
[2] S. J. Pearton, J. W. Corbett, and M. Stavola, *Hydrogen in Crystalline Semiconductors* (Spring-Verlag, Berlin, 1987).
[3] J. Weber and A. Mesli (Ed.), *Defects in Silicon: Hydrogen* (Elsevier Science, 1999).
[4] J. Weber, *Hydrogen in Semiconductors: From Basic Physics to Technology*, Phys. Stat. Sol. 5, 535 (2008).
[5] C. G. Van de Walle, and J. Neugebauer, *Hydrogen in Semiconductors*, *Ann. Rev. Mater. Res.* 36, 179 (2006).
[6] H. N. Waltenburg and J. T. Yates, Jr., Chem. Rev. 95, 1589 (1995).
[7] K. Oura, V. G. Lifshits, A. A. Saranin, A. V. Zotov, and M. Katayama, Surf. Sci. Rep. 35, 1 (1999).
[8] S. K. Jo, J. H. Kang, X.-M. Yang, J. M. White, J. G. Ekerdt, J. W. Keto, and J. Lee, *Direct Absorption of Gas-Phase Atomic Hydrogen by Si(100): A Narrow Temperature Window*, Phys. Rev. Lett. 85, 2144 (2000).
[9] J. Y. Maeng, S. Kim, S. K. Jo, W. P. Fitts, and J. M. White, *Absorption of Gas-Phase Atomic Hydrogen by Si(100): Effect of Surface Atomic Structures*, Appl. Phys. Lett. 79, 36 (2001).
[10] M. Jung and S. K. Jo, *Hydrogen Absorption by Si(100): Enhancement and Suppression by HF Etching*, J. Phys. Chem. C 115, 23463 (2011).
[11] S. K. Jo, *Preparation and Stability of Silyl Adlayers on 2x2-Reconstructred and Modified Si(100) Surfaces*, J. Kor. Vac. Soc. 18, 15 (2009).
[12] J. H. Kang, S. K. Jo, B. Gong, P. Parkinson, D. E. Brown, J. M. White, and J. G. Ekerdt, *Amorphization of Single-Crystalline Silicon by Thermal-Energy Atomic Hydrogen*, Appl. Phys. Lett. 75, 91 (1999).
[13] A.W. R. Leitch, A. Alex, and J. Weber, *Raman Spectroscopy of Hydrogen Molecules in Crystalline Silicon*, Phys. Rev. Lett. 81, 421 (1998).
[14] S. Pizzini, *Point Defects in Semiconductors*, Physical Chemistry of Semiconductor Materials and Processes (John Wiley & Sons, 2015) Chapter 2.
[15] J. J. Boland, *Hydrogen as a Probe of Semiconductor Surface Structure: The Ge(111)-c(2 X 8) Surface*, Science, 255, 186 (1992).
[16] J. Y. Maeng, J. Y. Lee, Y. E. Cho, S. Kim, and S. K. Jo, *Surface Dihydrides on Ge(100): A Scanning Tunneling Microscopy Study,* Appl. Phys. Lett. 19, 3555 (2002).
[17] J. Y. Lee, S. J. Jung, J. Y. Maeng, Y. E. Cho, S. Kim, and S. K. Jo, *Atomic-Scale Structural Evolution of Ge(100) Surfaces Etched by H and D,* Appl. Phys. Lett. 84, 5028 (2004).
[18] J. Y. Lee, J. Y. Maeng, A. Kim, Y. E. Cho, and S. Kim, *Kinetics of H_2 (D_2) Desorption from a Ge(100)-2x1:H(D) Surface Studied Using STM and TPD*, J. Chem. Phys. 118, 1929 (2003).
[19] P. W. Loscutoff and S. F. Bent, *Reactivity of the Germanium Surface: Chemical Passivation and Functionalization*, Ann. Rev. Phys. Chem. 57, 467 (2006).
[20] J. Weber, M. Hiller, and E. V. Lavrov, *Hydrogen in Germanium*, Mater. Sci. Semicond. Proc. 9, 564 (2006).
[21] R. Pillarisetty, *Academic and Industry Research Progress in Germanium Nanodevices*, Nature 479, 324 (2011).
[22] P. Ponath, K. Fredrickson, A. B. Posadas, Y. Ren, X. Wu, R. K. Vasudevan, M. B. Okatan, S. Jesse, T. Aoki, M. R. McCartney, D. J. Smith, S. V. Kalinin, K. Lai, and A. A. Demkov, *Carrier Density Modulation in a Germanium Heterostructure by Ferroelectric Switching*, Nature Comm. 6, 6067 (2015).
[23] S. Banerjee, C. H. Patterson, and J. F. McGilp, *Group V Adsorbate Structures on Vicinal Ge(001) Surface Determined from the Optical Spectrum*, Appl. Phys. Lett. 110, 233903 (2017).
[24] S. Hu, E. L. Lin, A. K. Hamze, A. Posadas, H. Wu, D. J. Smith, A. A. Demkov, and J. G. Ekerdt, *Zintl Layer Formation during Perovskite ALD on Ge(001)*, J. Chem. Phys. 146, 052817 (2017).
[25] J.-H. Lee, E. K. Lee, W.-J. Joo, Y. Jang, B.-S. Kim, J. Y. Lim, S.-H. Choi, S. J. Ahn, J. R. Ahn, M.-H. Park, C.-W. Yang, B. L. Choi, S.-W. Hwang, and D. Whang, *Wafer-Scale Growth of Single-Crystal Monolayer Graphene on Reusable Hydrogen-Terminated Germanium*, Science 344, 286 (2014).
[26] M. Walker, M. S. Tedder, J. D. Palmer, J. J. Mudd, and C. f. McConville, *Low Temperature Removal of Surface Oxides and Hydrocarbons form Ge(100) Using Atomic Hydrogen,* Appl. Surf. Sci. 379, 1 (2016).
[27] P. Ponath, A. B. Posada, and A. A. Demkov, *Ge(001) Surface Cleaning Methods for Device Integration*, Appl. Phys. Rev. 4, 021308 (2017).
[28] T. Nishimura, S. Kabuyanagi, W. Zhang, C. H. Lee, T. Yajima, K. Nagashio, and A. Toriumi, *Atomically Flat Planarization of Ge(100), (110), and (111) Surfaces in H_2 Annealing*, Appl. Phys. Express 7, 051301 (2014).
[29] S. V. Sivaram, H. Y. Hui, M. de la Mata, J. Arbiol, and M. A. Filler, *Surface Hydrogen Enables Subeutectic Vapor-Liquid-Solid Semiconductor Nanowire Growth*, Nano Lett. 16, 6717 (2016).
[30] M. Stavola, *Hydrogen in Silicon and Germanium*, The 5th International Symposium on Advanced Science and Technology of Silicon Materials (JSPS Si Symposium; Nov. 10-14, 2008, Kona, Hawaii, USA) Proceedings, pp. 337-343.
[31] S. K. Jo, B. Gong, G. Hess, J. M. White, and J. G. Ekerdt, *Low-Temperature Si(100) Etching: Facile Abstraction of SiH3(a) by Thermal Hydrogen Atoms,* Surf. Sci. Lett. 394, L162 (1997).
[32] M. Budde, B. B. Nielsen, C. P. Cheney, N. H. Tolk, and L. C. Feldmann, *Local Vibrational Modes of Isolated Hydrogen in Germanium,* Phys. Rev. Lett. 85, 2965 (2000).
[33] M. Stavola, *Hydrogen in Silicon and Germanium*, Proceedings of the 5th International Symposium on Advanced Science and Technology of Silicon Materials (JSPS Si Symposium) (Nov. 10-14, 2008; Hawaii, USA) pp. 337-343.